Memories of Opiate Withdrawal Emotional States Correlate with Specific Gamma Oscillations in the Nucleus Accumbens

Cyril Dejean[1,2,7,8], Mathieu Sitko[1,2,7], Paul Girardeau[1,2], Amine Bennabi[3,4], Stéphanie Caillé[1,2], Martine Cador[1,2], Thomas Boraud[5,6] and Catherine Le Moine*[,1,2]

[1]Université de Bordeaux, INCIA, UMR 5287, Bordeaux, France; [2]CNRS, INCIA, UMR 5287, Bordeaux, France; [3]Université de Bordeaux, I2M, UMR 5295, Bordeaux, France; [4]CNRS, I2M, UMR 5295, Bordeaux, France; [5]Université de Bordeaux, IMN, UMR 5293, Bordeaux, France; [6]CNRS, IMN, UMR 5293, Bordeaux, France

Affective memories associated with the negative emotional state experienced during opiate withdrawal are central in maintaining drug taking, seeking, and relapse. Nucleus accumbens (NAC) is a key structure for both acute withdrawal and withdrawal memories reactivation, but the NAC neuron coding properties underpinning the expression of these memories remain largely unknown. Here we aimed at deciphering the role of NAC neurons in the encoding and retrieval of opiate withdrawal memory. Chronic single neuron and local field potentials recordings were performed in morphine-dependent rats and placebo controls. Animals were subjected to an unbiased conditioned placed aversion protocol with one compartment (CS+) paired with naloxone-precipitated withdrawal, a second compartment with saline injection (CS−), and a third being neutral (no pairing). After conditioning, animals displayed a typical place aversion for CS+ and developed a preference for CS− characteristic of safety learning. We found that distinct NAC neurons code for CS+ or CS−. Both populations also displayed highly specific oscillatory dynamics, CS+ and CS− neurons, respectively, following 80 Hz (G80) and 60 Hz (G60) local field potential gamma rhythms. Finally, we found that the balance between G60 and G80 rhythms strongly correlated both with the ongoing behavior of the animal and the strength of the conditioning. We demonstrate here that the aversive and preferred environments are underpinned by distinct groups of NAC neurons as well as specific oscillatory dynamics. This suggest that G60/G80 interplay—established through the conditioning process—serves as a robust and versatile mechanism for a fine coding of the environment emotional weight.

Neuropsychopharmacology (2017) **42**, 1157–1168; doi:10.1038/npp.2016.272; published online 4 January 2017

INTRODUCTION

Through daily life experience, we learn to associate contexts and stimuli with emotions bearing positive or negative values. These affective memories underlie our ability to adapt to appetitive and aversive situations and play a crucial role in pathologies such as addiction. Indeed, conditioned drug-like and drug-opposite (eg, withdrawal) effects have been shown to play a crucial role in the development and maintenance of compulsive drug use (Milton and Everitt, 2012; Torregrossa *et al*, 2011). Opiate abuse in particular (heroin, morphine) induces a strong dependence that is characterized by the appearance of a withdrawal syndrome upon drug use cessation (Frenois *et al*, 2005a). Opiate withdrawal can induce a mild to severe somatic syndrome together with the formation of long-lasting aversive memories driven by the association of stimuli, contexts, and emotions related to withdrawal itself (Frenois *et al*, 2005a). In parallel to these negative associative memories, morphine-dependent subjects can also distinguish cues and contexts that consistently signal the absence of withdrawal and form associative memories based on these perceived safety signals (Caille *et al*, 2003; Leknes *et al*, 2011). Such emotional memories are considered as a key component in the addiction process in that they motivate drug seeking and further promote maladaptive behaviors such as sustained drug taking or relapse in abstinent subjects (Milton and Everitt, 2012; Torregrossa *et al*, 2011). Moreover, preclinical studies have shown that reactivation of affective memories associated with opiate withdrawal state can reinstate drug seeking (Hellemans *et al*, 2006a, b; Kenny *et al*, 2006).

The nucleus accumbens (NAC) is a 'limbic-motor inter-face' that underpins the production of adaptive behavioral responses (Carlezon and Thomas, 2009). The NAC subserves addictive processes by allowing the formation of specific representations of the sensory, emotional, and motivational properties of drug-associated stimuli or contexts that contribute to drive maladaptive behaviors characterizing

addiction (Cador et al, 1989; Robbins et al, 1989). Interestingly NAC is at stake for both the rewarding effects of opiates (Kelsey et al, 1989; Olds, 1982) and the aversive effects of withdrawal (Frenois et al, 2002, 2005a, b; Koob et al, 1989; Stinus et al, 1990). NAC neuron differential activity has been linked to both reward and aversion (see, eg, Roitman et al, 2010; Setlow et al, 2003), but little is known about the NAC precise coding of positive and negative in the frame of opiate dependence and withdrawal. Rate coding has been proposed as a model of dual coding for drug-related safety and aversion with tonic inhibition or excitation respectively (for review, see Carlezon and Thomas, 2009). Alternative mechanisms like neural codes based on spike train dynamics such as temporal or phase coding have been largely overlooked in the frame of opiate addiction. Synchronous theta and 4 Hz oscillatory activity in the limbic system is associated with successful reward retrieval (Benchenane et al, 2010; Fujisawa and Buzsaki, 2011) and most importantly in associative aversive memories, prefrontal cortex-amygdalar theta and 4 Hz oscillatory synchronization are instrumental for fear expression (Courtin et al, 2014; Dejean et al, 2016; Karalis et al, 2016). Oscillatory activity in the NAC and striatum and most particularly in the gamma band (40–120 Hz) is entrained by prefrontal and amygdalar oscillatory inputs (Donnelly et al, 2014; von Nicolai et al, 2014). Hence, beside rate coding, oscillatory synchronization in the gamma band appears as strong candidate mechanism for the behavioral expression of drug-related memories. In line with this idea, we have recently shown that chronic morphine and withdrawal were associated with specific modifications in NAC gamma band oscillations (40–120 Hz) in rodents (Dejean et al, 2013). In both morphine-dependent and -naive animals, these gamma oscillations split into two distinct functional frequency bands that have also been identified as candidate mechanisms in different memory-based paradigms (Headley and Pare, 2013; van der Meer et al, 2010). A specific increase in 60 Hz low gamma (G60) is observed during acute and chronic opiate stimulation, whereas 80 Hz high gamma (G80) is upregulated at the time of acute withdrawal (Dejean et al, 2013).

As G60 and G80 oscillations are acutely modulated by opiates and withdrawal (Dejean et al, 2013), the present work investigates their role in the expression of specific behaviors related to opiate withdrawal memories: (1) withdrawal itself but also (2) the preference associated with the absence of withdrawal. Using single unit and local field potential (LFP) recordings in a conditioned place aversion paradigm in behaving rats, we show here that aversion and preference are correlated with a differential activity of NAC neurons, and that in both spike trains and LFP, this functional scheme emerges from specific interactions between G60 and G80.

MATERIALS AND METHODS

Animals

Twelve male Sprague-Dawley rats (Charles River Laboratories, France) were individually housed under an inverted 12 h light/dark cycle at $21 \pm 2\,°C$ with food and water available *ad libitum*. Weight varied from 250 to 300 g at the beginning of the study to 300 to 350 g at the time of the last

recording. Surgical and experimental procedures were performed in accordance with the European Community's Council Directive (EU Directive 2010/63/EU86) for the care and use of laboratory animals. The present experiment was approved by the local animal care and use committee (approval 5012049-A).

Electrode Implantation Surgery

Rats were implanted with four independently moveable tetrodes in the NAC as described in Dejean et al (2013). Briefly, surgery took place after at least 7 days of daily handling, under full general gas anesthesia (Isoflurane 1.5–2%). The recording electrodes were lowered to position through small craniotomies above the structure. Six stainless-steel skull screws were inserted and the implant was affixed to the skull with super bond and dental acrylic. After the surgery, animals were injected with carboprofen (2 mg/kg, s.c.) for pain management and allowed to recover from anesthesia before being returned to the animal housing facilities where pain management was carried on for 5–7 days.

Behavioral Paradigm: Opiate Withdrawal Place Aversion Conditioning

Following the first surgery, morphine dependence was induced by subcutaneous implantation of two morphine ($n = 7$) or placebo ($n = 5$) pellets as previously described (Dejean et al, 2013). Withdrawal was precipitated by a naloxone injection (15 μg/kg s.c.) that induced a strong aversive state with mild somatic signs (Frenois et al, 2002). Place aversion conditioning took place in an unbiased Y-maze with three compartments as previously described in detail (Frenois et al, 2005b) (see also Figure 1a). Following a pretest, animals underwent conditioning during that rats received a saline injection on days 5, 7, and 9, and a naloxone injection (15 μg/kg) on alternate days (6, 8, and 10) before being placed in one compartment of the Y-maze for 20 min. The testing phase (test) involved a free Y-maze exploration for 20 min and a place aversion score was calculated as the difference between the percentage of time spent in the same compartment during test and pretest. The occurrence of some withdrawal signs (defecation and diarrhea) were analyzed by a visual inspection of the video recording. For a detailed description of the paradigm, see Supplementary Methods.

Behavioral and Electrophysiological Recordings

Behavior was monitored with a videotracking system (Plexon, TX, USA). NAC single units and LFP were recorded using Multichannel Acquisition Processor (MAP, Plexon). The wide band signal (0.1–9000 Hz) collected by the electrodes was amplified (×1000) before being digitized (40000 Hz sampling rate for single unit and 1000 Hz for LFP). Single units were manually sorted and cluster isolation was tested for significance (Offline sorter, Plexon). Units were classified as putative projection neurons or interneurons (Supplementary Figure S2a) using combined spike width and firing rate methods as previously described (Dejean et al, 2013). Behavioral and electrophysiological
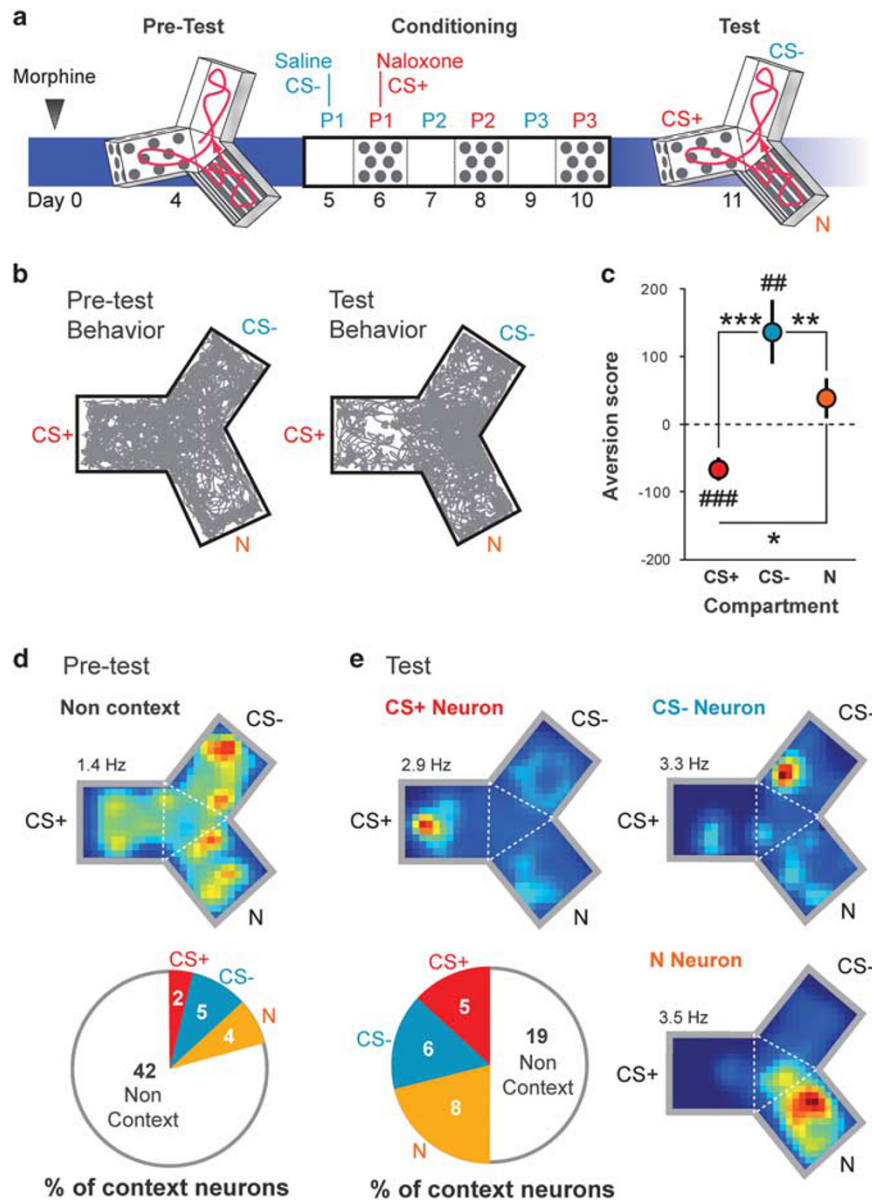
Figure 1 NAC neurons encode negative and positive emotional contexts after place aversion conditioning. (a) Place aversion conditioning took place in an unbiased Y-maze. At 4 days after morphine pellet implantation, rats underwent a pretest during which they freely explored the Y-maze for 20 min. During conditioning rats received saline injections (days 5, 7, and 9) or naloxone (days 6, 8, and 10) and were confined in a compartment for 20 min. P1, P2, and P3 stand for first, second, and third pairing with Saline/CS − (blue) first or Naloxone/CS+ (red). Test phase consisted in a free exploration of the Y-maze for 20. (b) Examples of behavior during exploration of the Y-maze in pretest and test. Gray lines represent the animal track during an entire session. (c) Aversion and place preference scores after conditioning. When compared with pretest, animals in test spent significantly less time in CS+ (Naloxone) compartment and more time in CS − (Saline) compartment (one sample *t*-test, n = 7, compartment *vs* zero % change, t(6) = 9.537, [##]p < 0.01 and t(6) = 4.218, [###]p < 0.001, respectively). No change was observed in neutral compartment (N). The percentage of time spent in compartment also significantly differed between CS+ and CS − (one way RM ANOVA, n = 7, F(2) = 23.6, p < 0.001, Holm–Sidak *post hoc*, CS+ *vs* CS−: q(2) = 6.851, p < 0.001; CS − *vs* N: q(2) = 3.929, p < 0.01; CS+ *vs* N: q(2) = 2.921, *p < 0.05, **p < 0.01, ***p < 0.001. (d) During pretest, the vast majority of NAC neurons did not display any firing preference for a specific compartment. Top example shows the firing rate (color coded) of a neuron as a function of the animal position during pretest session. This typical neuron fired in all three compartments. Cells with such profile represented ∼ 79% of pretest sample (bottom pie-chart, noncontext neuron, 42/53), whereas only 21% displayed firing peaks restricted to one compartment (context neurons, 11/53). (e) During test, a strong increase in the amount of context neurons coding for CS+ (top left example), CS − (top right example), and N (bottom right example) was observed with their overall proportion significantly rising to 50% (19/38, χ^2, pretest *vs* test, χ^2(1) = 7.293, p < 0.01). No significant bias toward one compartment was found whether it was in pretest or test (χ^2(2) = 0.786 in pretest, χ^2(2) = 0.158 in test, p > 0.05). Error bars: mean ± SEM.

activities were monitored daily from pretest to test. Some animals displayed brief sleep episodes by the end of the pretest period. Although these events were sparse, for the sake of rigor and to avoid such epochs to influence our analysis, we isolated and removed those episodes showing behavioral (eg, prolonged immobility) and electrophysiological hallmarks of sleep (eg, changes in LFP slow oscillatory regime).

Electrophysiological Data Analysis

Frequency firing maps were computed combining spike sorting and tracking results. An image containing the Y-maze was divided into 1024 pixels (32×32). Sorted spikes were distributed in the maze space according to the animal position at the time of firing. The firing rate in each pixel was calculated as the ratio of the number of spikes fired inside the pixel over the time spent by the animal in the same pixel along the entire session (Figures 1d and e). Firing was Z-scored and pixels showing a significantly Z-score (> 1.96) and six contiguous significant pixels defined a firing field. Neurons displaying one or more clusters in a single compartment of the maze were tagged as context neurons.

The phase relationship between spikes and LFP was investigated using phase histograms. For each rhythm of interest, LFP were band pass filtered in Matlab and the phase of filtered signals was extracted by calculating the Hilbert transform of the signal in Matlab (The Mathworks, MA, USA). Spike-phase histograms were tested for homogeneity (Rayleigh test), with a nonhomogeneous histogram indicating significant phase locking. LFP power spectrum analyses revealed an overlap between G60 and G80 event frequency bands. To overcome this problem and perform a specific analysis of these two types of events, each single gamma event was precisely isolated and classified as G60 or G80 (see Supplementary Methods and Supplementary Figure S3). To predict the animal position based on the presence of G60 and G80 events in the LFP, we used a machine learning approach and a naive Bayes classifier and assessed prediction accuracy through ROC analysis (see Supplementary Methods).

Statistics

For each statistical analysis, Kolmogorov–Smirnov normality test was first performed. To calculate the appropriate sample size, power analyses were carried out to determine the number of rats needed (Sigmaplot, Systat, Germany) using a power > 0.8 and a type I error threshold $\alpha = 0.05$. Two-sided parametric statistical tests were used in case data met normality and homoscedasticity. In case one or both of these conditions were not fulfilled, or the sample size was small (5 or 6), nonparametric methods were used. On one occasion, equal variance criteria were not met and no nonparametric alternative was available to our knowledge (Figure 4b). These results are thus only provided for information. In case of multiple comparisons, adjustments were systematically done to control for family errors (Holm–Sidak and Tukey's *post hoc* tests for parametric and nonparametric statistics respectively). Experimenter blinding (single blind) was used on one occasion: the experimenter extracting the firing fields of neurons in the maze had no knowledge of the animal ID or the condition (test or pretest). On graphics, error bars are mean $\pm$ SEM unless otherwise stated.

RESULTS

NAC Neuron Firing Correlates with Negative and Positive Emotional Contexts after Place Aversion Conditioning

Unbiased place conditioning resulted in a marked aversion toward the withdrawal-associated compartment (CS+, Figures 1b and c). Interestingly, every animal also developed a preference for the saline paired compartment (CS −, Figures 1b and c), whereas the time spent in neutral compartment (N) remained unchanged. In placebo animals the time spent in compartments in test and pretest did not change (Supplementary Figure S1a). Hence, familiarity regarding CS+ and CS − acquired during conditioning does not explain test behavior in morphine animals nor can saline injection explain the preference toward CS −. This shows that place conditioning, in addition to allocating a negative emotional weight to the CS+, also established the maze as a robust bivalent emotional environment with CS − becoming a positively perceived compartment. Moreover, the investigation of motion statistics revealed that the distribution of animal speeds remained unchanged between pretest and test in placebo or morphine animals (Supplementary Figure S1d). Similarly, the total distance traveled during a session was unaffected by the experimental group or the conditioning (Supplementary Figure S1e). NAC is crucial for the association of actions with their values. We therefore investigated the electrophysiological correlates of NAC cells with the different contexts and most particularly the CS+ and CS −. We focused on putative medium spiny projection neurons (Supplementary Figure S2) and recorded and analyzed 258 cells (pretest: $n = 53$; conditioning: $n = 167$; test $n = 38$). In pretest, activity of most neurons was evenly distributed in space with firing fields observed in two or three compartments (79%; 42/53, Figure 1d). During test a majority of cells started to fire specifically in one of the three emotional contexts (50%, 19/38, Figure 1e). Among them similar amounts presented firing fields restricted to CS+, CS − or N (5/19, 6/19, and 8/19, respectively). Note that at the population level, average firing rate was not found to be modulated by conditioning, NAC substructure (core or shell), or compartment (Supplementary Figure S2d). In placebo animals (Supplementary Figures S2e and f), NAC presented similar proportions of context neurons in pretest (4/19, 21%) and test (7/29, 24%). When comparing with morphine animals, these values did not differ from pretest but were significantly lower than that observed during test (Fisher's exact test, placebo pretest *vs* morphine pretest: $p = 0.94$; placebo test *vs* morphine pretest: $p = 1$; placebo pretest *vs* morphine test: $p < 0.05$; placebo test *vs* morphine test: $p < 0.05$). These data correlate with a switch from a weakly emotional context in pretest to the emotional polarization of the maze observed after conditioning (test).

Slow and Fast Gamma Event Relative Weight Correlates with Preference and Aversion

The analysis of LFP revealed a striking homology between the animals' preference or aversion behavior and gamma band oscillations. Gamma oscillation events occurred under the form of distinct spindles that could be classified into two categories based on their main frequency component
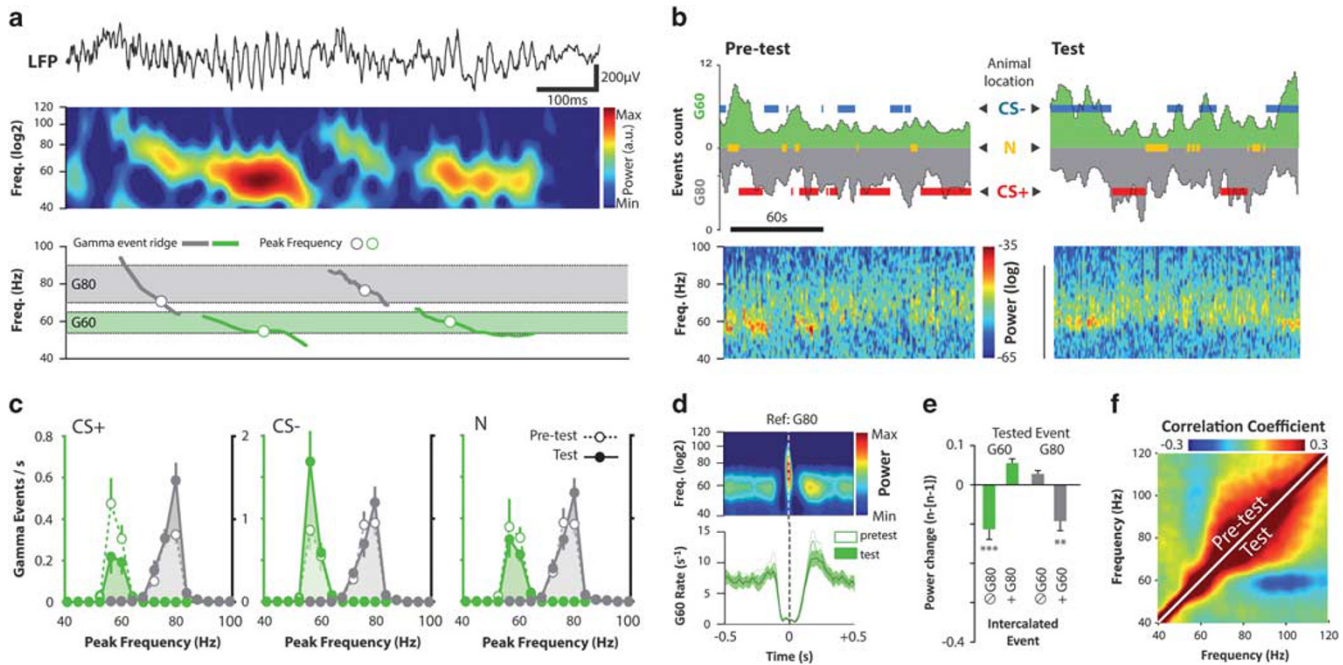
Figure 2 Slow and fast gamma bands occurrence and interactions are differentially affected by conditioned withdrawal. (a, top) Raw LFP trace in the nucleus accumbens (NAC). (a, center) Time-resolved gamma band wavelet spectrum showing discrete 60 or 80 Hz events. Note frequency is plotted with a log2 scale. (a, bottom) Spectrogram ridge represents the frequency at which the power is maximal for consecutive time points within individual G60 (green) and G80 (grey) events. Shaded areas highlight the frequency bands used for G60 (55–65 Hz) and G80 (70–90 Hz) event detection (see Supplementary Methods). (b, top) Time-resolved G60 and G80 event rates (bin: 1 s) with superimposed animal location (CS+, CS −, or N; note that center is not displayed). (b, bottom) Corresponding time-resolved gamma band FFT spectrum (bin size 1 s). (c) Distribution of discretized peak frequency G60 (green) and G80 (gray) events in pretest and test as a function of compartment (frequency bin: 3.75 Hz). No change in frequency distribution was observed in any condition (Kolmogorov–Smirnov two-sample tests, $n = 7$, KS dist = 0.238 for G60, KS dist = 0.189 for G80, $p > 0.05$ in both cases) or in peak frequency between pretest and test (G60, pretest: 58.454 ± 0.159 Hz, range: 58.053–59.212 Hz; test: 58.459 ± 0.236, range: 57.683–59.579 Hz; paired t-test; $t(6) = -0.0218$, $p > 0.05$; G80, pretest: 77.628 ± 0.382 Hz, range: 76.427–79.156 Hz; test: 77.774 ± 0.309, range: 76.266–78.733 Hz; paired t-test; $t(6) = -0.457$, $p > 0.05$). (d, top) Perievent time gamma-band spectrogram. (d, bottom) Peri-event time histogram for G60 events centered on G80 events in pretest and test. Note the interaction between both types of events as G60 events are more likely to occur after a G80 event than before either in pretest or test. (e) Power is changing from one event to the next depending on the presence or absence of an intercalated event from the other range. The power of G60 event increases from event n to event $n+1$ if a G80 event occurs between them. Conversely, the power of G80 events decreases if a G60 event is intercalated between events n and $n+1$ ($n = 14$, paired t-test; G60: $t(13) = 4.607$, **$p < 0.01$, G80: $t(13) = 3.845$, ***$p < 0.001$). (f) Cross-frequency Spearman's correlation averaged across pretest and test conditions. Although power positively correlates for neighboring frequencies (diagonal), G60 and G80 powers present a negative correlation.

(Figure 2a and Supplementary Figures S3c and d): the G60 and G80 rhythms with power peaking near 60 and 80 Hz, respectively. These rhythms have been observed in both morphine and drug-free subjects (Dejean *et al*, 2013; van der Meer *et al*, 2010) and, strikingly, in our paradigm their relative prevalence was tightly linked to the animal's behavior. During epochs spent in aversive CS+ G60 event probability and duration decreased, whereas G80 probability increased (Figures 2b and c and Supplementary Figures S3e and S4a). In the preferred CS − instead, G60 events were strongly promoted and both their duration and power increased compared with pretest (Figures 2b and c, Supplementary Figures S3e and S4a, c). Interestingly, no changes were observed in N for either frequency component. These opposed yet concurrent changes in G60 and G80 suggest that both rhythms are involved in the coding of the compartment emotional value. Further analysis revealed that the probability to observe a G60 event turned out to be higher after the occurrence of a G80 event (Figure 2d) and power was significantly increased from one G60 event to the next when a G80 event occurred in between them (Figure 2e). Conversely, the probability to observe a G80

event was lower after the occurrence of a G60 event and power decreased from one G80 event to the next with an intercalated G60 events (Figure 2e). These results suggest a possible fast interaction between G60 and G80. In line with this, cross-frequency coupling analysis at the scale of an entire recording session shows that power of ~ 60 Hz was negatively correlated with that ~ 80 Hz (Figure 2f). Interestingly, this negative correlation was strengthened by conditioning (pretest rho $= -0.069 \pm 0.015$, test: rho $= -0.196 \pm 0.0349$, paired t-test, $t(6) = 3.763$, $p < 0.01$). Recent works have emphasized that NAC gamma rhythms correlate with the animal's motoric behavior (Malhotra *et al*, 2015). In our experiment, although G60 and G80 events were indeed found to be correlated with rats' motoric activity (Supplementary Figures S5a–c), their fluctuations were significantly better explained by their mutual interactions (Supplementary Figures S5a–c). Moreover, at the level of a whole session, gamma ratio was not correlated to the motoric activity of the animal (Supplementary Figure S5d). Altogether, these findings show a strong relationship between task conditioning and G60 and G80 event probabilities. The strengthening between pretest and test phase suggests that
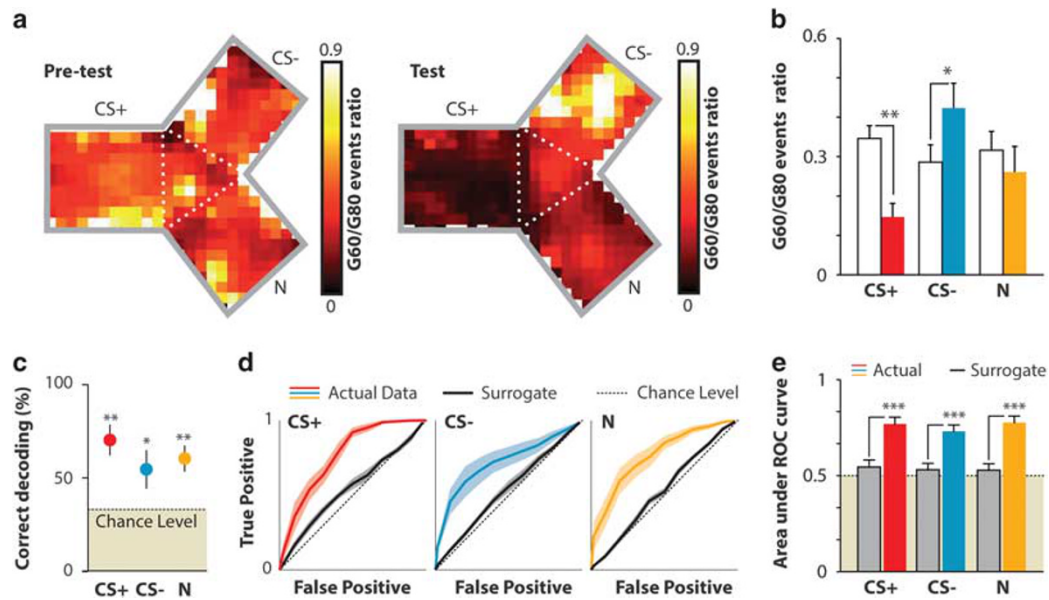
Figure 3 G60 and G80 events interplay predicts animal behavior. (a) Gamma ratio as a function of animal position averaged across animals in pretest and test phase. Although no specific patterns emerge during test, after conditioning, CS+ compartment is characterized by an overall bias toward G80 (negative gamma index) and toward G60 for CS − (positive gamma index). (b) Effect of conditioning on gamma. Analysis of gamma ratio (G60/G80 probability) in CS+, CS −, and N (empty bars: pretest; filled bars: test) shows that conditioning promotes G80 over G60 in CS+ and conversely promotes G60 compared with G80 in CS −. No effect of conditioning was observed for N (two-way repeated measure ANOVA test; $n = 7$; Factor 1: Context, $F_{(2, 14)} = 2.416$, $p > 0.05$; Factor 2; pretest *vs* test, $F_{(1, 7)} = 0.472$, $p > 0.05$, F1 × F2: $F_{(2, 14)} = 9.7$, $p < 0.01$, Holm–Sidak *post hoc* test, pretest *vs* test within CS+: $t_{(6)} = 2.902$, within CS −: $t_{(6)} = 2.185$, within N: $t_{(6)} = 0.812$, **$p < 0.01$, *$p < 0.05$). (c) Mean percentage of correct decoding of animals' positions compared with chance level (33.3% occupancy, one sample unilateral *t*-test, CS+: $p < 0.01$; CS −: $p < 0.05$; N: $p < 0.05$). (d) Receiver operating characteristic (ROC) analysis for actual and surrogate data (×1000 shuffle of animal's positions). (e) Quantification area under ROC curves compared with that of chance level (0.5) and surrogate data (two-way ANOVA test; $n = 7$; Factor 1: Context, $F_{(2, 14)} = 0.331$, $p > 0.05$; Factor 2; actual *vs* surrogate data, $F_{(1, 7)} = 62.234$, $p < 0.001$, F1 × F2: $F_{(2, 14)} = 0.775$, $p > 0.05$, Holm–Sidak *post hoc* test, actual *vs* surrogate data within CS+: $t_{(6)} = 4.350$, $p < 0.001$, within CS −: $t_{(6)} = 4.161$, $p < 0.001$, within N: $t_{(6)} = 5.173$, $p < 0.001$, ***$p < 0.001$). Error bars represent mean ± SEM.

more than events themselves, their relative prevalence could be a marker of the context emotional value. To quantify this relationship in our task, we calculated the ratio between G60 and G80 event probabilities in the different compartments (Figure 3a) and quantified the change in gamma ratio between pretest and test phases (Figure 3b). In pretest phase, gamma event ratio was similar in all three compartments. During the test, gamma ratio decreased in CS+ and increased in CS − (Figures 3a and b), whereas no change could be observed in N. Gamma event ratio is therefore linked to the animal emotional state during the test session. As aversion, preference, and emotional neutrality are associated with specific compartments after conditioning, we hypothesized that the relative weight of G60 and G80 events at a given time during test should be predictive of the animal's location. To test this hypothesis we applied a spatial decoding algorithm based on the relative presence of G60 and G80 events inside discrete time bins and found that the animal's location could be predicted with significant success in any of the three compartments (Figures 3c–e). Thus, in the NAC of morphine-dependent animals, G60 and G80 events—and most specifically their relative prevalence— stand as a potential vector underlying aversion and preference associated with opiate withdrawal and its absence, respectively.

Neurons Firing for Aversion and Preference Are Locked to Specific LFP Gamma Rhythms

The modulation of neuronal activity by G60 or G80 proved to be a robust marker of preference or aversion behaviors in our task. Joint spike–LFP analysis revealed that context neuron spiking inside the neuron firing field were often coincidental with the occurrence of G80 events for CS+ neurons (eg, Figure 4a) or G60 events for CS − neurons (eg, Figure 4b). The quantification of gamma ratio inside CS+ and CS − neuron firing fields confirmed those observations as CS+ neurons displayed a significantly lower ratio in firing field compared with CS − neurons (eg, Figure 4c). Context neuron firing was not only coincidental with gamma events occurrence as their fine temporal dynamics were also modulated according to gamma rhythm (Figure 4d). In pretest and test, several units phase locked on G60 (pretest: 27/53, test: 21/38) and/or G80 (pretest: 16/53, test: 15/38, Figures 4d–f). Surprisingly, despite changes observed in LFP gamma power, G60 and G80 overall phase locking did not differ in pretest and test. However, when considering specifically the subpopulation of context neurons characterized during test phase, G80 phase locking was highly specific of CS+ neurons inside the CS+ compartment (Figures 4d and g), mirroring the increase in G80 event occurrence and the decrease of G60/G80 ratio that indicates G80 prevalence. Conversely, CS − neurons preferentially locked on G60 oscillations while the animal
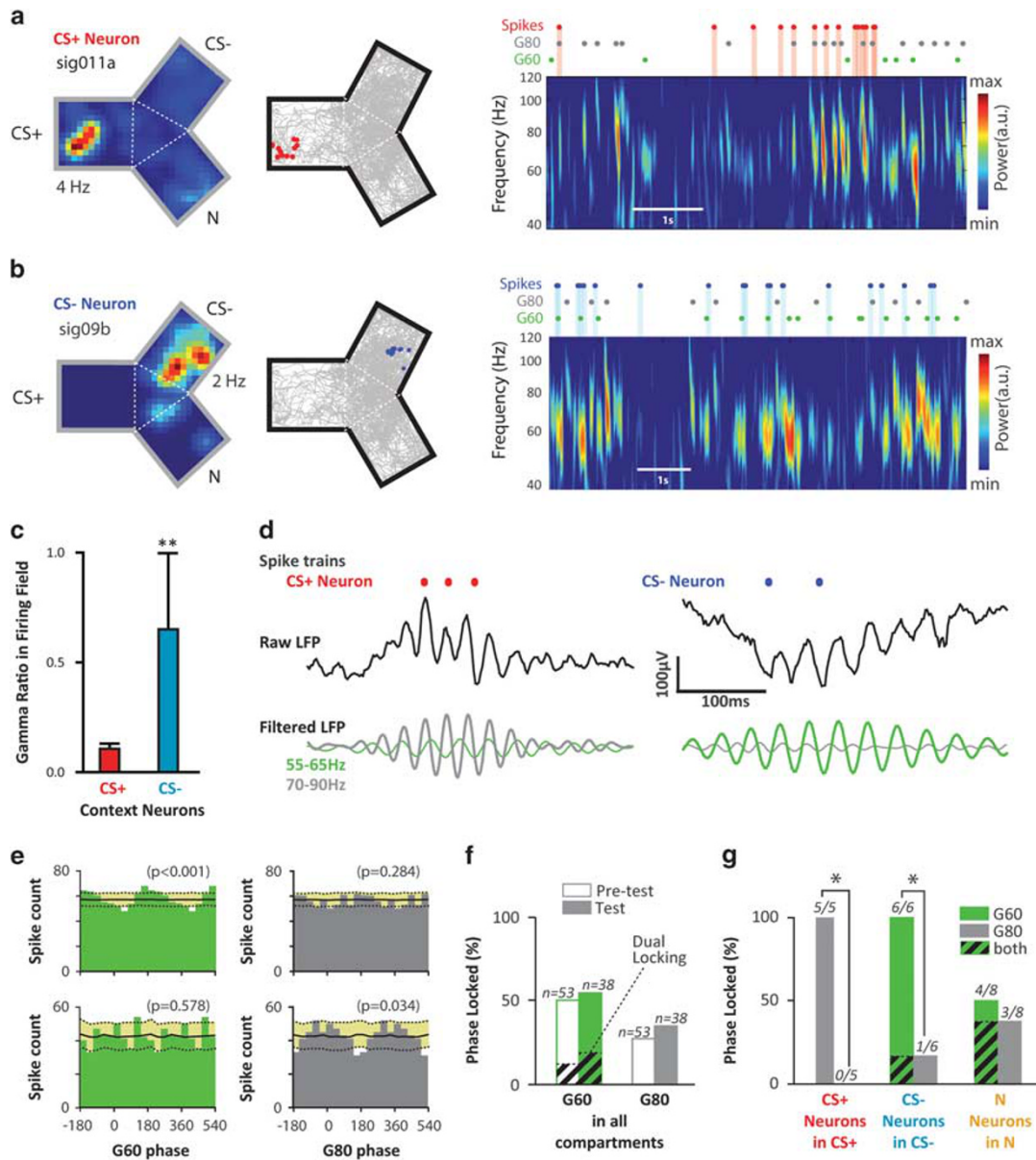
Figure 4 Context neuron activity is locked to specific LFP gamma rhythms. (a, b) Examples of CS+ (a) and CS− context neurons (b). Left: firing rate as a function of animal position. Middle: firing sequence within firing field (blue and red dots: spikes) superimposed on the global animal track (gray lines). Right: Time-resolved firing activity, G80 and G60 event occurrence, and corresponding spectrogram during the same sequence as above. (c) Gamma ratio in firing field. Gamma ratio within firing field averaged across all CS+ (red) and CS− context neurons (blue). Gamma ratio was significantly higher for CS− neurons compared with CS+ (Mann–Whitney test, $U = 3.00$, $n = 5$ for CS+ neurons; $n = 6$ for CS− neurons, **$p < 0.01$). Error bars represent mean ± SEM. (d) Example raster of simultaneous spike–LFP recordings for neurons displayed in (a) and (b). (e) G60 and G80 oscillations modulate single neuron activity in the NAC. Each row represents the spike-phase histograms for the two different neurons exemplified in (a), (b), and (d). They were respectively modulated by G60 in the 55–65 Hz range (top, Rayleigh test, G60: $p < 0.001$, G80: $p = 0.284$) or G80 in the 70–90 Hz range (bottom, Rayleigh test, G60: $p = 0.578$, G80: $p < 0.05$). The black line represents chance level defined as the average spike count as a function of phase for surrogate data (yellow area: 95% confidence interval of the mean). (f) Overall percentage of neuron phase locked to G60 and G80 (Fisher's exact test, pretest *vs* test, $p > 0.05$ for both G60 and G80). (g) Compartment and gamma-band specific modulation of context neuron phase locking in test condition. CS+ neurons are exclusively modulated by G80 rhythm in the CS+ compartment (left, gray bar). CS− neurons are preferentially modulated by G60 in the CS− compartment (center, green bar). N neurons displayed entrainment for both G60 and G80 (right) with a high level of double locking (3 out of 4 cells). *Significant difference between G60 and G80 percentage of locked neurons within a particular compartment (Fisher's exact test, $p < 0.05$).

was inside CS− (Figure 4g), matching the increase in both G60 event occurrence and gamma ratio. Although N neurons displayed significant G60 or G80 phase locking, we did not observe any preferred phase locking toward one or the other rhythm (Figure 4g). Spike–LFP analyses

hence revealed a tight binding between context neurons, their preferred compartment, and gamma oscillations with a clear bimodal pattern related to emotional values: aversion and preference are associated with G80 and G60, respectively.
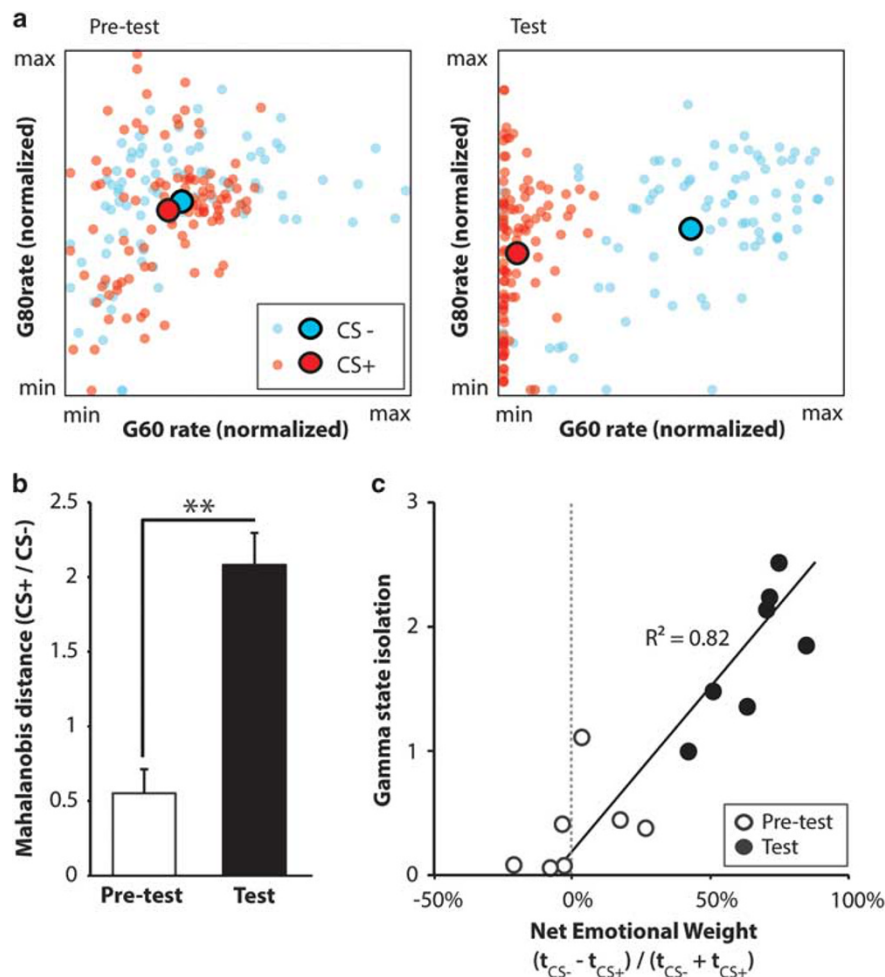
Figure 5 NAC gamma states in aversive and safe compartments correlate with animal's behavior. (a) Gamma state diagram (G60 *vs* G80 event rates in compartment) in pretest and test conditions for a single animal example (light color points: single pixel; large points, black outline: cluster centroid). The rate of gamma events is normalized to the respective minima and maxima of G60 and G80 occurrence rate across all animals. (b) Average Mahalanobis distance between CS − and CS+ clusters (error bar: SEM; paired *t*-test, $n = 7$; $t(6) = -4.507$, $**p < 0.01$). (c) Net emotional weight of the maze as a function of the isolation of CS+ and CS − gamma states. Net emotional weight of the maze is the difference in time spent in CS − *vs* CS+ divided by the total amount of time spent in both compartments in a given recording session in pretest or test. The isolation between CS+ and CS − gamma event states is quantified by the part of Mahalanobis distance comprised between the lower boundaries of CS+ and CS − distribution confidence intervals (see Supplementary Methods).

NAC Gamma Events in Aversive and Preferred Compartments Correlate with the Strength of Associative Learning

Because G60 and G80 may, depending on their balance, code either positive or negative emotional states, we hypothesized that the relative weight of G60 and G80 rates at a given location of the maze (referred to as gamma state from here) in NAC represents the net emotional value of this location. To test this postulate, we first compared gamma states in CS+ and CS − . During pretest, CS+ and CS − gamma states were largely overlapping (Figure 5a), whereas in conditioned animals CS+ and CS − gamma states represented significantly isolated clusters (Figure 5a). Consequently, the average Mahalanobis distance between CS+ and CS − clusters was significantly larger in test phase (Figure 5b). We then quantified the magnitude of CS+ and CS − gamma state isolation by calculating the significant part of their Mahalanobis distance that is the distance between CS+ and CS − confidence intervals. Gamma state isolation was used

as an index for the strength of emotional coding and compared with the strength of the conditioning (net emotional value, see Materials and Methods). We found a striking positive correlation between gamma state isolation and the net emotional value of the maze (Figure 5c), suggesting that the strength of bidirectional gamma activity is a direct reflection of the strength of emotional associative learning.

Establishment of Aversion and Preference Coding Through Gamma Oscillations During Conditioning

During conditioning the experience of acute withdrawal in CS+ is aversive *per se* as confirmed by the presence of typical withdrawal signs during naloxone pairings such as enhanced defecations and diarrhea (Figure 6a). Interestingly, diarrhea occurrence (a hallmark of withdrawal signs) also increased during conditioning suggesting a sensitization to repeated naloxone injections (Figure 6a). However, it is not clear how
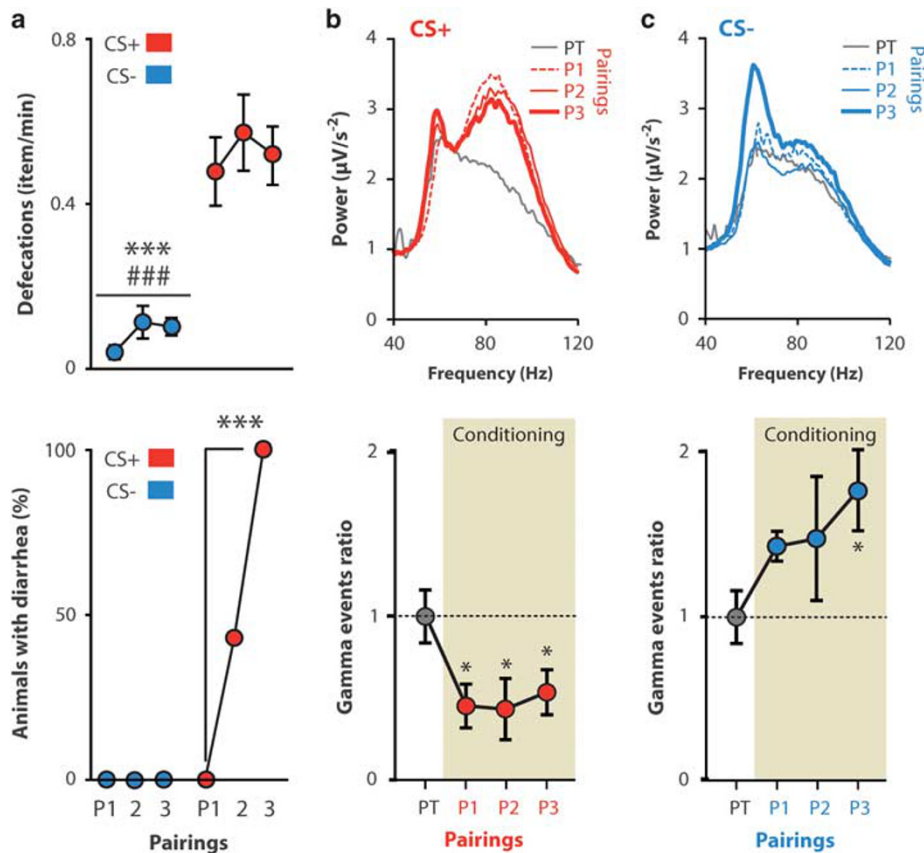
Figure 6 Establishment of gamma oscillation profiles during conditioning. (a, top) Defecation rate was significantly higher during all three withdrawal (CS+) pairings compared with saline (CS−) pairings (two-way ANOVA test; $n = 7$; Factor 1: treatment, $F_{(1, 2)} = 53.208$, ***$p < 0.001$; Factor 2: pairing, $F_{(2, 2)} = 0.614$, $p > 0.05$, F1 × F2: $F_{(2, 14)} = 0.044$, $p > 0.05$, Holm–Sidak *post hoc* test, CS+ *vs* CS−, P1: $t(6) = 5.369$, P2: $t(6) = 4.873$, P3: $t(6) = 4.410$, ###$p < 0.001$ for all pairings). (a, bottom) The amount of rats displaying diarrhea was null in saline pairings (CS−) but appeared with naloxone by P2 and increased significantly throughout withdrawal subsequent pairings (Fisher's exact test, P1 *vs* P3: ***$p < 0.001$). (b, c, top) Power spectral density averaged across animals for the different pairings (b/red: Naloxone/CS+ pairings P1 to P3, c/blue: saline/CS− pairings P1 to P3). (b, c, bottom) Gamma ratio averaged across animals for the different treatment exposure (b/red: Naloxone/CS+, c/blue: Saline/CS−). Note that values are normalized on pretest level (one-way RM ANOVA on ranks tests; $n = 7$ for CS+ and CS−; CS+: $\chi^2(3) = 9.4$, $p < 0.05$, Tukey's *post hoc* test, pretest *vs* P1: $q(6) = 4.111$, pretest *vs* P2: $q(6) = 4.111$, control *vs* P3: $q(6) = 3.795$, *$p < 0.05$ in the three cases; CS−: $\chi^2(3) = 11.4$, $p = 0.01$, Tukey's *post hoc* test, pretest *vs* P1: $q(6) = 2.858$, pretest *vs* P2: $q(6) = 2.887$, pretest *vs* P3: $q(6) = 3.795$, *$p < 0.05$ for P3 only).

CS− acquires its positive emotional value and how electrophysiological correlates of preference develop during conditioning. A general assumption is that through consecutive CS+ and CS− pairings a subject progressively learns to associate CS− with the absence of negative outcome (safety learning). Based on this, we postulated that safety coding through gamma event ratio profile should develop throughout the conditioning phase, whereas aversion coding should be present from the first naloxone-CS+ pairing. To test this, we analyzed LFP gamma events (Figures 6b and c) in the three consecutive CS+ and CS− pairing sessions along the conditioning phase (see protocol, Figure 1a). The investigation of electrophysiological data across CS+ pairings revealed a decrease in gamma ratio compared with pretest (Figure 6b) that was immediate (pairing 1, P1) and conserved in subsequent pairings. Conversely, confinement in the CS− resulted in a progressive increase in gamma ratio (Figure 6c) that was found significant only by P3. Importantly, these changes in gamma ratio were mirrored by changes in gamma phase locking of single neurons (Supplementary Figure S6). Overall, these results confirm

that aversion-related gamma pattern is present from the first pairing of CS+ with naloxone withdrawal, whereas the preference-related pattern for its part is absent in the first stages of conditioning and emerges from the repetition of CS−/saline and CS+/naloxone associations.

DISCUSSION

The present study shed light on NAC neuronal activity that could underlie the expression of aversion and preference for opiate-related emotional memories. The interest of this question stems from the crucial role of those memories in drug seeking and relapse, and the involvement of NAC in their behavioral expression (Koob and Volkow, 2010; Milton and Everitt, 2012). Our work shows that although the context associated with drug withdrawal is perceived as aversive as expected, a second context specifically characterized by the absence of withdrawal can be progressively perceived as positive. During test, at the time these emotional memories are expressed, distinct groups of NAC neurons and specific oscillatory dynamics correlate with the position of the animal

in the aversive or preferred environment. Indeed, the firing pattern of neurons underlying preference and aversion are driven by slow (G60) and fast (G80) gamma band oscillations, respectively. Finally, the relative weight and the moment-to-moment interactions between both rhythms precisely define the emotional value allocated to discrete locations of the environment through the conditioning process.

A substantial amount of NAC neurons displayed spatial and emotional information in their spike trains. Hence, just as in drug-naive animals (Hayes *et al*, 2014; Khamassi *et al*, 2008; Lansink *et al*, 2012; Schmitzer-Torbert *et al*, 2005), single NAC medium spiny neurons encode spatial and emotional traits of the opiate-dependent animal's context. Importantly, distinct neuronal subpopulations were found to match aversive and preferred locations. This functional segregation shows that the NAC encodes both aversion and preference in dependent-animals just as in drug-naive subjects as evidenced with associative learning based on naturally aversive or rewarding stimuli in both rodents (Roitman *et al*, 2010) and humans (Levita *et al*, 2009). Interestingly, a recent work has highlighted that different populations of dynorphin cells in the dorsal or ventral part of the NAC shell may code for preference and aversion, respectively (Al-Hasani *et al*, 2015). Even if our recordings span across both core and shell, and are mainly dorsal, our data further support the idea that neuronal subpopulations of the NAC may specifically underlie place conditioning for positive and negative emotional values. Thus, NAC activity may subserve representations of contextual elements that are crucial for adapted behaviors (Lansink *et al*, 2012; Schmitzer-Torbert *et al*, 2005) including spatiotemporal features and emotional traits whichever their value. In the frame of addiction, such functional flexibility may be required to drive behavior (1) towards the drug and its rewarding properties, (2) towards a beacon of safety, or (3) away from contexts associated with negative aspects of drug abuse (eg, withdrawal). Our paradigm models these last two aspects but cannot directly address questions related to the substance rewarding properties. As our chronic morphine treatment induced tolerance (Gold *et al*, 1994), it is likely that preference for the CS − compartment (also previously shown in Caille *et al*, 2003 with the same naloxone dose) develops with the progressive perception of the absence of withdrawal as an increasing safety signal. Preclinical studies have shown that conditioned opiate withdrawal reinstate morphine conditioned place preference (Lu *et al*, 2005) and reactivation of opiate withdrawal memories indeed plays a role in drug seeking (Hellemans *et al*, 2006a, b; Kenny *et al*, 2006). Together with the present results, slow gamma role in CS − could also underpin the drive of a dependent animal toward opiate consumption as shown for cocaine intake (Carelli and Wondolowski, 2003). Experiments of opiate self-administration would thus be of great interest to test this hypothesis.

The specific dynamics of context neurons suggests that temporal coding through gamma oscillations in NAC supports the expression of aversion and preference in morphine-dependent animals. Gamma state could provide a dynamic representation of emotional state as well as a fine index of the strength of emotional learning in opiate-dependent rats. When confronted with complex or conflicting environmental features, gamma interplay could underpin the production of behavior finely adapted to the animal's ever-changing environment. Interestingly, in a spatial task rewarded by food, gamma oscillations in a band very similar to that of G60 have been associated with reward retrieval, whereas faster oscillations of ∼ 80 Hz were related to high uncertainty about the reward (van der Meer and Redish, 2009). Hence, similar electrophysiological signatures are shared by reward uncertainty and withdrawal-bound aversion (G80) but also by reward delivery and safety in the absence of withdrawal (G60). Given this presence of oscillations in the G60 and G80 bands in drug-naive animals, such mechanism could well be generalized as a physiological encoding process for emotional memories.

The aversion for the withdrawal compartment is a straight-forward and classic behavioral outcome in this associative learning paradigm (Frenois *et al*, 2005a). Moreover, all animals also displayed a clear preference for the compartment associated with saline injection as shown previously (Caille *et al*, 2003). In classical fear conditioning studies in drug-naive animals, the absence of negative outcome following a neutral stimulus is also known to lead to safety learning and specific neurophysiological responses (Genud-Gabai *et al*, 2013; Likhtik *et al*, 2014). During conditioning, physiological signs (enhanced defecation and diarrhea) were immediately correlated with the G80 signature, suggesting that aversion coding directly depends on naloxone effect. CS − pattern was different, as G60 signature developed over successive pairings. This suggests that CS − acquisition of a positive, safe emotional value is progressive. One possible explanation lies in the profound homeostatic changes observed in the limbic system of morphine-dependent subjects (Koob and Le Moal, 2008) in which neurophysiological balance relies on the presence of the drug (Dejean *et al*, 2013). Here, the loss of this balance upon opioid receptor blockade in CS+ pairings is repeatedly opposed to the stability experienced within CS − where a drug-dependent steady state is fueled by the continuous morphine stimulation. We therefore propose that the repetition of withdrawal absence is progressively perceived and encoded as a positive signal that confers CS − the properties of a safety context.

Our study highlights a candidate oscillatory mechanism supporting aversion and preference coding in NAC neurons. At the scale of the brain, synchronized oscillations are widely accepted as a powerful mechanism to bind distant structure activities and functions (Fell and Axmacher, 2011). NAC-projecting basolateral amygdala (BLA) and medial prefrontal cortex (mPFC) are two critical structures for associative and emotional memories (Cardinal *et al*, 2002) and mPFC, BLA, and NAC dynamic interactions are central in emotional memories and their expression (Ambroggi *et al*, 2008; Karalis *et al*, 2016; Klavir *et al*, 2013; Livneh and Paz, 2012; Popescu *et al*, 2007; Stuber *et al*, 2011). Specific oscillatory mechanisms in these structures have been shown to underpin fear (Bauer *et al*, 2007; Courtin *et al*, 2014; Dejean *et al*, 2016; Popa *et al*, 2010), appetitive conditioning (Popescu *et al*, 2009), and could also support discrimination of fear and safety signals (Likhtik *et al*, 2014). In opiate-dependent rats, mPFC, BLA, and NAC synchronize in delta, theta, and gamma frequency bands (Dejean *et al*, 2013) and are activated during the retrieval of opiate withdrawal memory

(Frenois et al, 2005b; Lucas et al, 2012). Long-range oscillatory synchronization inside mPFC–BLA–NAC network of dependent animals could therefore support the formation and expression of emotional memories linked to opiate withdrawal. Considering the crucial role of these memories in the maintenance of drug consumption and relapse, understanding network-scale, dynamic mechanisms behind their formation and recall could lead to refined therapeutic approaches for drug addiction.

AUTHOR CONTRIBUTIONS

CD and PG performed the experiments. CD, MS, and AB analyzed the data. CD, CLM, SC, MC, and TB designed the experiments and contributed to the interpretation of the data. CD, MS, and CLM wrote the paper.

REFERENCES

Al-Hasani R, McCall JG, Shin G, Gomez AM, Schmitz GP, Bernardi JM et al (2015). Distinct subpopulations of nucleus accumbens dynorphin neurons drive aversion and reward. Neuron 87: 1063–1077.

Ambroggi F, Ishikawa A, Fields HL, Nicola SM (2008). Basolateral amygdala neurons facilitate reward-seeking behavior by exciting nucleus accumbens neurons. Neuron 59: 648–661.

Bauer EP, Paz R, Pare D (2007). Gamma oscillations coordinate amygdalo-rhinal interactions during learning. J Neurosci 27: 9369–9379.

Benchenane K, Peyrache A, Khamassi M, Tierney PL, Gioanni Y, Battaglia FP et al (2010). Coherent theta oscillations and reorganization of spike timing in the hippocampal- prefrontal network upon learning. Neuron 66: 921–936.

Cador M, Robbins TW, Everitt BJ (1989). Involvement of the amygdala in stimulus-reward associations: interaction with the ventral striatum. Neuroscience 30: 77–86.

Caille S, Stinus L, Espejo EF, De Deurwaerdere P, Spampinato U, Koob GF (2003). Inhibition of 5-HT neurotransmission increases clonidine protective effects on naloxone-induced conditioned place aversion in morphine-dependent rats. Neuropsychopharmacology 28: 276–283.

Cardinal RN, Parkinson JA, Hall J, Everitt BJ (2002). Emotion and motivation: the role of the amygdala, ventral striatum, and prefrontal cortex. Neurosci Biobehav Rev 26: 321–352.

Carelli RM, Wondolowski J (2003). Selective encoding of cocaine versus natural rewards by nucleus accumbens neurons is not related to chronic drug exposure. J Neurosci 23: 11214–11223.

Carlezon WA Jr, Thomas MJ (2009). Biological substrates of reward and aversion: a nucleus accumbens activity hypothesis. Neuropharmacology 56(Suppl 1): 122–132.

Courtin J, Chaudun F, Rozeske RR, Karalis N, Gonzalez-Campo C, Wurtz H et al (2014). Prefrontal parvalbumin interneurons shape neuronal activity to drive fear expression. Nature 505: 92–96.

Dejean C, Boraud T, Le Moine C (2013). Opiate dependence induces network state shifts in the limbic system. Neurobiol Dis 59: 220–229.

Dejean C, Courtin J, Karalis N, Chaudun F, Wurtz H, Bienvenu T et al (2016). Prefrontal neuronal assemblies temporally control fear behaviour. Nature 535: 420–424.

Donnelly NA, Holtzman T, Rich PD, Nevado-Holgado AJ, Fernando AB, Van Dijck G et al (2014). Oscillatory activity in the medial prefrontal cortex and nucleus accumbens correlates with impulsivity and reward outcome. PLoS One 9: e111300.

Fell J, Axmacher N (2011). The role of phase synchronization in memory processes. Nat Rev Neurosci 12: 105–118.

Frenois F, Cador M, Caille S, Stinus L, Le Moine C (2002). Neural correlates of the motivational and somatic components of naloxone-precipitated morphine withdrawal. Eur J Neurosci 16: 1377–1389.

Frenois F, Le Moine C, Cador M (2005a). The motivational component of withdrawal in opiate addiction: role of associative learning and aversive memory in opiate addiction from a behavioral, anatomical and functional perspective. Rev Neurosci 16: 255–276.

Frenois F, Stinus L, Di Blasi F, Cador M, Le Moine C (2005b). A specific limbic circuit underlies opiate withdrawal memories. J Neurosci 25: 1366–1374.

Fujisawa S, Buzsaki G (2011). A 4 Hz oscillation adaptively synchronizes prefrontal, VTA, and hippocampal activities. Neuron 72: 153–165.

Genud-Gabai R, Klavir O, Paz R (2013). Safety signals in the primate amygdala. J Neurosci 33: 17986–17994.

Gold LH, Stinus L, Inturrisi CE, Koob GF (1994). Prolonged tolerance, dependence and abstinence following subcutaneous morphine pellet implantation in the rat. Europ J Pharmacol 253: 45–51.

Hayes DJ, Duncan NW, Xu J, Northoff G (2014). A comparison of neural responses to appetitive and aversive stimuli in humans and other mammals. Neurosci Biobehav Rev 45C: 350–368.

Headley DB, Pare D (2013). In sync: gamma oscillations and emotional memory. Front Behav Neurosci 7: 170.

Hellemans KG, Dickinson A, Everitt BJ (2006a). Motivational control of heroin seeking by conditioned stimuli associated with withdrawal and heroin taking by rats. Behav Neurosci 120: 103–114.

Hellemans KG, Everitt BJ, Lee JL (2006b). Disrupting reconsolidation of conditioned withdrawal memories in the basolateral amygdala reduces suppression of heroin seeking in rats. J Neurosci 26: 12694–12699.

Karalis N, Dejean C, Chaudun F, Khoder S, Rozeske RR, Wurtz H et al (2016). 4-Hz oscillations synchronize prefrontal-amygdala circuits during fear behavior. Nat Neurosci 19: 605–612.

Kelsey JE, Carlezon WA Jr., Falls WA (1989). Lesions of the nucleus accumbens in rats reduce opiate reward but do not alter context-specific opiate tolerance. Behav Neurosci 103: 1327–1334.

Kenny PJ, Chen SA, Kitamura O, Markou A, Koob GF (2006). Conditioned withdrawal drives heroin consumption and decreases reward sensitivity. J Neurosci 26: 5894–5900.

Khamassi M, Mulder AB, Tabuchi E, Douchamps V, Wiener SI (2008). Anticipatory reward signals in ventral striatal neurons of behaving rats. Eur J Neurosci 28: 1849–1866.

Klavir O, Genud-Gabai R, Paz R (2013). Functional connectivity between amygdala and cingulate cortex for adaptive aversive learning. *Neuron* **80**: 1290–1300.

Koob GF, Le Moal M (2008). Review. Neurobiological mechanisms for opponent motivational processes in addiction. *Philos Trans R Soc Lond B Biol Sci* **363**: 3113–3123.

Koob GF, Stinus L, Le Moal M, Bloom FE (1989). Opponent process theory of motivation: neurobiological evidence from studies of opiate dependence. *Neurosci Biobehav Rev* **13**: 135–140.

Koob GF, Volkow ND (2010). Neurocircuitry of addiction. *Neuropsychopharmacology* **35**: 217–238.

Lansink CS, Jackson JC, Lankelma JV, Ito R, Robbins TW, Everitt BJ *et al* (2012). Reward cues in space: commonalities and differences in neural coding by hippocampal and ventral striatal ensembles. *J Neurosci* **32**: 12444–12459.

Leknes S, Lee M, Berna C, Andersson J, Tracey I (2011). Relief as a reward: hedonic and neural responses to safety from pain. *PLoS One* **6**: e17870.

Levita L, Hare TA, Voss HU, Glover G, Ballon DJ, Casey BJ (2009). The bivalent side of the nucleus accumbens. *Neuroimage* **44**: 1178–1187.

Likhtik E, Stujenske JM, Topiwala MA, Harris AZ, Gordon JA (2014). Prefrontal entrainment of amygdala activity signals safety in learned fear and innate anxiety. *Nat Neurosci* **17**: 106–113.

Livneh U, Paz R (2012). Amygdala-prefrontal synchronization underlies resistance to extinction of aversive memories. *Neuron* **75**: 133–142.

Lu L, Chen H, Su W, Ge X, Yue W, Su F *et al* (2005). Role of withdrawal in reinstatement of morphine-conditioned place preference. *Psychopharmacology (Berl)* **181**: 90–100.

Lucas M, Frenois F, Cador M, Le Moine C (2012). Remodeling of the neuronal circuits underlying opiate-withdrawal memories following remote retrieval. *Neurobiol Learn Mem* **97**: 47–53.

Malhotra S, Cross RW, Zhang A, van der Meer MA (2015). Ventral striatal gamma oscillations are highly variable from trial to trial, and are dominated by behavioural state, and only weakly influenced by outcome value. *Eur J Neurosci* **42**: 2818–2832.

Milton AL, Everitt BJ (2012). The persistence of maladaptive memory: addiction, drug memories and anti-relapse treatments. *Neurosci Biobehav Rev* **36**: 1119–1139.

Olds ME (1982). Reinforcing effects of morphine in the nucleus accumbens. *Brain Res* **237**: 429–440.

Popa D, Duvarci S, Popescu AT, Lena C, Pare D (2010). Coherent amygdalocortical theta promotes fear memory consolidation during paradoxical sleep. *Proc Natl Acad Sci USA* **107**: 6516–6519.

Popescu AT, Popa D, Pare D (2009). Coherent gamma oscillations couple the amygdala and striatum during learning. *Nat Neurosci* **12**: 801–807.

Popescu AT, Saghyan AA, Pare D (2007). NMDA-dependent facilitation of corticostriatal plasticity by the amygdala. *Proc Natl Acad Sci USA* **104**: 341–346.

Robbins TW, Cador M, Taylor JR, Everitt BJ (1989). Limbic-striatal interactions in reward-related processes. *Neurosci Biobehav Rev* **13**: 155–162.

Roitman MF, Wheeler RA, Tiesinga PH, Roitman JD, Carelli RM (2010). Hedonic and nucleus accumbens neural responses to a natural reward are regulated by aversive conditioning. *Learn Mem* **17**: 539–546.

Schmitzer-Torbert N, Jackson J, Henze D, Harris K, Redish AD (2005). Quantitative measures of cluster quality for use in extracellular recordings. *Neuroscience* **131**: 1–11.

Setlow B, Schoenbaum G, Gallagher M (2003). Neural encoding in ventral striatum during olfactory discrimination learning. *Neuron* **38**: 625–636.

Stinus L, Le Moal M, Koob GF (1990). Nucleus accumbens and amygdala are possible substrates for the aversive stimulus effects of opiate withdrawal. *Neuroscience* **37**: 767–773.

Stuber GD, Sparta DR, Stamatakis AM, van Leeuwen WA, Hardjoprajitno JE, Cho S *et al* (2011). Excitatory transmission from the amygdala to nucleus accumbens facilitates reward seeking. *Nature* **475**: 377–380.

Torregrossa MM, Corlett PR, Taylor JR (2011). Aberrant learning and memory in addiction. *Neurobiol Learn Mem* **96**: 609–623.

van der Meer MA, Kalenscher T, Lansink CS, Pennartz CM, Berke JD, Redish AD (2010). Integrating early results on ventral striatal gamma oscillations in the rat. *Front Neurosci* **4**: 300.

van der Meer MA, Redish AD (2009). Low and high gamma oscillations in rat ventral striatum have distinct relationships to behavior, reward, and spiking activity on a learned spatial decision task. *Front Integr Neurosci* **3**: 9.

von Nicolai C, Engler G, Sharott A, Engel AK, Moll CK, Siegel M (2014). Corticostriatal coordination through coherent phase-amplitude coupling. *J Neurosci* **34**: 5938–5948.